

The synthesis and structural characterization of bis(mercaptoimidazolyl)(pyrazolyl)hydroborato and tris(mercaptoimidazolyl)hydroborato complexes of thallium(I) and thallium(III)

Clare Kimblin, Brian M. Bridgewater, Tony Hascall and Gerard Parkin *

Department of Chemistry, Columbia University, New York, New York 10027, USA

Received 2nd December 1999, Accepted 22nd February 2000

Published on the Web 31st March 2000

The bis(mercaptoimidazolyl)(pyrazolyl)hydroborato and tris(mercaptoimidazolyl)hydroborato ligands, $[\text{pzBm}^{\text{Me}}]^-$ and $[\text{Tm}^{\text{Ph}}]^-$, have been used to prepare complexes of both thallium(I) and thallium(III), namely $[\text{pzBm}^{\text{Me}}]\text{Tl}$, $[\text{pzBm}^{\text{Me}}]\text{TlMe}_2$, $\{[\text{Tm}^{\text{Ph}}]_2\text{Tl}\}_2$ and $\{[\text{Tm}^{\text{Ph}}]_2\text{Tl}\}[\text{ClO}_4]$. For example, reaction of $[\text{pzBm}^{\text{Me}}]\text{Tl}$ with Me_2TlCl yields $[\text{pzBm}^{\text{Me}}]\text{TlMe}_2$, while reaction of $[\text{Tm}^{\text{Ph}}]\text{Li}$ with $\text{Tl}(\text{ClO}_4)_3$ yields $\{[\text{Tm}^{\text{Ph}}]_2\text{Tl}\}[\text{ClO}_4]$. $[\text{pzBm}^{\text{Me}}]\text{TlMe}_2$, $\{[\text{Tm}^{\text{Ph}}]_2\text{Tl}\}_2$ and $\{[\text{Tm}^{\text{Ph}}]_2\text{Tl}\}[\text{ClO}_4]$ have been structurally characterized by X-ray diffraction. Interestingly, for the monomeric thallium(III) derivatives, the pyrazolyl group does not coordinate to the thallium center in the dimethyl complex $[\text{pzBm}^{\text{Me}}]\text{TlMe}_2$, which is therefore four-coordinate, whereas all the mercaptoimidazolyl groups coordinate to thallium in $\{[\text{Tm}^{\text{Ph}}]_2\text{Tl}\}^+$, thereby resulting in a six-coordinate octahedral geometry.

Introduction

Following Reglinski's use of 2-mercapto-1-methylimidazole to prepare the $[\text{S}_3]$ tripodal tris(2-mercapto-1-methylimidazolyl)borate ligand, $[\text{Tm}^{\text{Me}}]^-$,¹⁻³ we have synthesized related derivatives with bulky aryl substituents, namely the phenyl and mesityl analogs $[\text{Tm}^{\text{Ph}}]^-$ and $[\text{Tm}^{\text{Mes}}]^-$ (Fig. 1).⁴ In terms of both the method of synthesis and their tripodal nature, these ligands may be considered to be sulfur counterparts of the extensively studied tris(pyrazolyl)borate ligand system.⁵ Furthermore, we have also synthesized a hybrid $[\text{S}_2\text{N}]$ ligand that incorporates both pyrazolyl and mercaptoimidazolyl donors, $[\text{pzBm}^{\text{Me}}]^-$ (Fig. 1).⁶ Thallium complexes, and particularly Tl^{I} derivatives, feature prominently as transfer reagents in the applications of these poly(mercaptoimidazolyl)- and poly(pyrazolyl)borate ligands.^{5b,d} In this paper we report the synthesis and structural characterization of not only Tl^{I} complexes, but also Tl^{III} derivatives, namely the four-coordinate dimethyl complex $[\text{pzBm}^{\text{Me}}]\text{TlMe}_2$ and the six-coordinate sandwich complex $\{[\text{Tm}^{\text{Ph}}]_2\text{Tl}\}[\text{ClO}_4]$.

Results and discussion

(i) Synthesis and structural characterization of $[\text{pzBm}^{\text{Me}}]\text{ZnMe}$ and $[\text{pzBm}^{\text{Me}}]\text{TlMe}_2$

The thallium(I) derivative of the hybrid $[\text{S}_2\text{N}]$ ligand, $[\text{pzBm}^{\text{Me}}]^-$, may be obtained by treatment of the lithium complex $[\text{pzBm}^{\text{Me}}]\text{Li}^6$ with $\text{Tl}(\text{O}_2\text{CMe})$ in methanol (Scheme 1). As expected by analogy to poly(pyrazolyl)borate chemistry,^{5d} $[\text{pzBm}^{\text{Me}}]\text{Tl}$ is a convenient reagent for the synthesis of the zinc methyl complex $[\text{pzBm}^{\text{Me}}]\text{ZnMe}$ via reaction with Me_2Zn (Scheme 1). Since mononuclear tetrahedral zinc complexes with a $[\text{S}_2\text{N}]$ donor array are rare, due to the proclivity of sulfur to bridge,⁷ the molecular structure of $[\text{pzBm}^{\text{Me}}]\text{ZnMe}$ (Fig. 2) was determined by X-ray diffraction, thereby demonstrating that it does exist as a simple mononuclear complex, analogous to the iodide derivative, $[\text{pzBm}^{\text{Me}}]\text{ZnI}$.⁶ The Zn–C bond length in $[\text{pzBm}^{\text{Me}}]\text{ZnMe}$ [1.988(4) Å] is comparable to that in the related three-coordinate complex $[\text{Bm}^{\text{Me}}]\text{ZnMe}$ [1.97(1) Å],⁸ and also to those in the four-coordinate tris(pyrazolyl)borate derivatives $[\text{Tp}^{\text{Me}_2}]\text{ZnMe}$ [1.981(8) Å],⁹ $[\text{Tp}^{\text{Bu}}]\text{ZnMe}$ [1.971(4) Å],⁹ $[\text{Tp}^{\text{Ph}}]\text{ZnMe}$ [1.950(4) Å],¹⁰ and $[\text{PhTp}^{\text{Bu}}]\text{ZnMe}$ [1.994(2) Å].¹¹

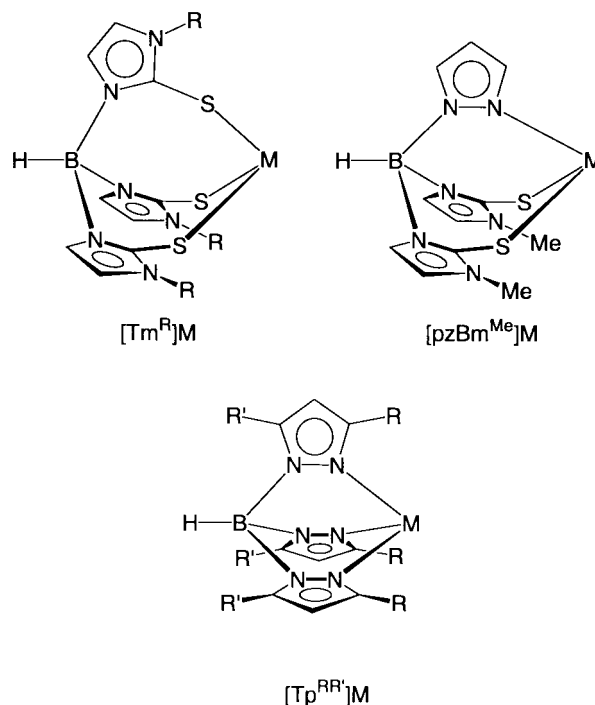
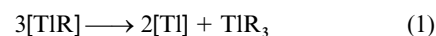
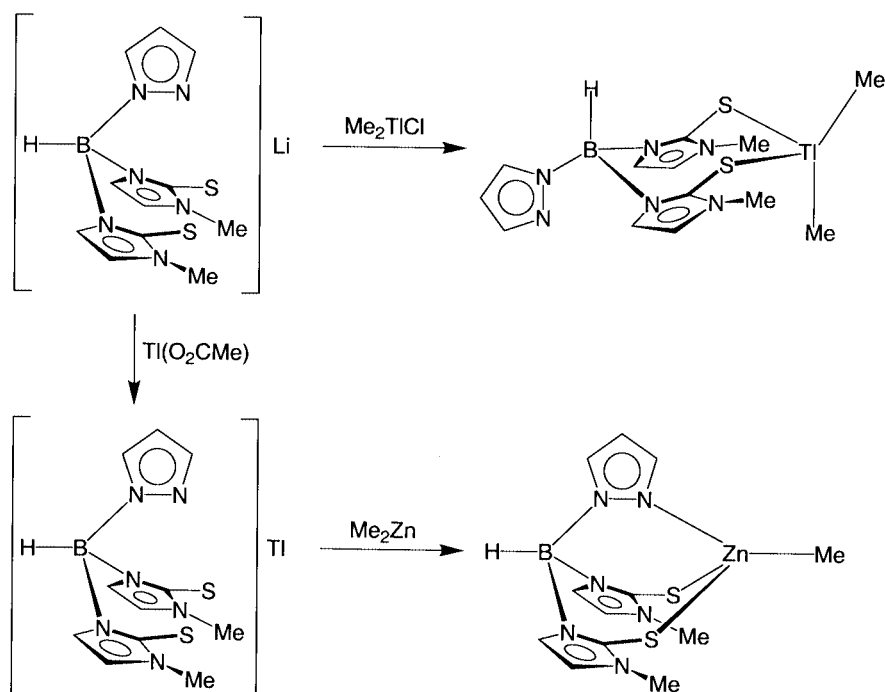


Fig. 1 Tridentate $[\text{Tm}^{\text{R}}]$, $[\text{pzBm}^{\text{Me}}]$, and $[\text{Tp}^{\text{RR}'}]$ ligands.

The effectiveness of Tl^{I} complexes as ligand transfer reagents in reactions with metal alkyls, R_nM , is commonly attributed to the driving force associated with the decomposition of the resulting Tl^{I} alkyl, which results in deposition of elemental thallium.¹² In this regard, it has long been known that the reaction of Tl^{I} with one equivalent of MeLi yields Me_3Tl and Tl , presumably as a result of disproportionation of unstable $[\text{MeTl}]$ (eqn. (1)).¹³



We have now obtained additional evidence which supports this proposed disproportionation for $[\text{TlR}]$. Specifically, we have observed that, with prolonged reaction times, the Tl^{III}



Scheme 1

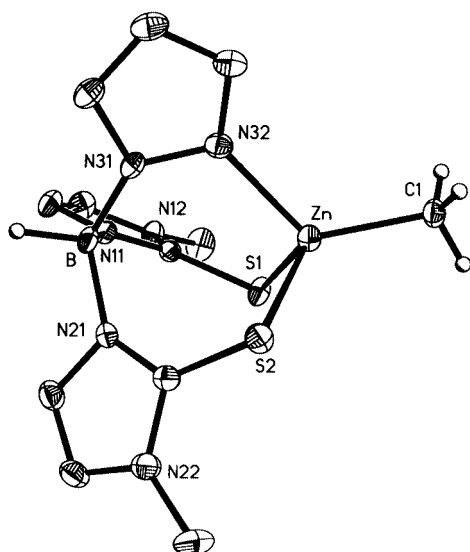


Fig. 2 Molecular structure of $[\text{pzBm}^{\text{Me}}]\text{ZnMe}$. Selected bond lengths (Å) and angles ($^{\circ}$): Zn–S(1) 2.404(1), Zn–S(2) 2.410(1), Zn–N(32) 2.043(4), Zn–C(1) 1.988(4); S(1)–Zn–S(2) 107.24(5), S(1)–Zn–N(32) 102.7(1), S(2)–Zn–N(32) 92.6(1), S(1)–Zn–C(1) 111.7(2), S(2)–Zn–C(1) 117.0(1), N(32)–Zn–C(1) 123.1(2).

complex $[\text{pzBm}^{\text{Me}}]\text{TlMe}_2$ is formed as a by-product in the reaction of $[\text{pzBm}^{\text{Me}}]\text{Tl}$ with Me_2Zn . More conveniently, however, $[\text{pzBm}^{\text{Me}}]\text{TlMe}_2$ may be obtained by the direct reaction of $[\text{pzBm}^{\text{Me}}]\text{Tl}$ with TlMe_2Cl (Scheme 1), and its molecular structure has been determined by X-ray diffraction (Fig. 3). Significantly, and in contrast to the zinc methyl complex $[\text{pzBm}^{\text{Me}}]\text{ZnMe}$, only the sulfur donors coordinate to the thallium center in $[\text{pzBm}^{\text{Me}}]\text{TlMe}_2$.

Structurally characterized dimethyl thallium complexes are well known, and include those that also feature coordination of a bidentate $[\text{S}_2]$ donor ligand, as illustrated in Table 1. The sulfur ligands that have been previously studied in this respect, however, are mainly of the type $[\text{X}]\text{S}_2$, where X contains a single atom bridge between the sulfur donors. As such, these ligands generate complexes with four-membered $[\text{XS}_2\text{Tl}]$ chelate rings, in contrast to the “chair-like” 8-membered ring that is present in $[\text{pzBm}^{\text{Me}}]\text{TlMe}_2$. The Tl–C bond lengths of 2.150(3) Å and

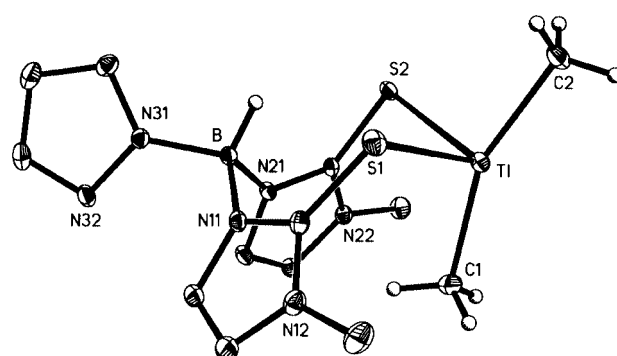


Fig. 3 Molecular structure of $[\text{pzBm}^{\text{Me}}]\text{TlMe}_2$. Selected bond lengths (Å) and angles ($^{\circ}$): Tl–C(1) 2.150(3), Tl–C(2) 2.152(3), Tl–S(1) 2.754(1), Tl–S(2) 2.7266(8); C(1)–Tl–C(2) 157.7(2), C(1)–Tl–S(2) 99.7(1), C(2)–Tl–S(2) 97.2(1), C(1)–Tl–S(1) 97.6(1), C(2)–Tl–S(1) 94.6(1), S(1)–Tl–S(2) 97.44(3).

2.152(3) Å for $[\text{pzBm}^{\text{Me}}]\text{TlMe}_2$ are comparable to the mean value of 2.11 Å for structurally characterized thallium methyl complexes listed in the Cambridge Structural Database.¹⁴

For further comparison, the Tl–C bond lengths for other dimethyl thallium complexes that also feature bidentate sulfur ligands are summarized in Table 1. A noteworthy aspect of all the structurally characterized complexes listed in Table 1 is that the C–Tl–C bond angles deviate strongly from the tetrahedral value, with some approaching linearity. Analysis of the Cambridge Structural Database¹⁴ indicates that expansion of the C–M–C bond angle in tetrahedral dialkyl complexes is a general trend for the Group 13 elements: B, Al, Ga, In and Tl (Table 2). For example, such a trend is observed for bis-(pyrazolyl)borate complexes, $[\text{Bp}^{\text{RR}}]\text{MMe}_2$ (M = B, Al, Ga, In),^{15,16} although a thallium derivative is yet to be structurally characterized for this series.¹⁷

It is also worth noting that the bidentate coordination of the $[\text{pzBm}^{\text{Me}}]$ ligand differs somewhat from those of the other sulfur ligands listed in Table 1. For example, the average Tl–S bond length of 2.74 Å in $[\text{pzBm}^{\text{Me}}]\text{TlMe}_2$ is substantially shorter than that for the majority of the other complexes, for which the average Tl–S bond length is 2.94 Å,¹⁸ a notable exception, however, is $[\text{Pr}^n_2\text{NCS}_2]\text{TlMe}_2$ which has a Tl–S bond length of 2.75 Å which is comparable to that for $[\text{pzBm}^{\text{Me}}]\text{TlMe}_2$.

Table 1 Metrical and NMR spectroscopic data for [S₂]TlMe₂ complexes

	<i>d</i> (Tl–C)/Å	C–Tl–C°	<i>d</i> (Tl–S _{av})/Å	S–Tl–S°	¹ <i>J</i> _{Tl–C} /Hz	² <i>J</i> _{Tl–H} /Hz	Ref.
[pzBm ^{Me}]TlMe ₂	2.15	157.7	2.74	97.4	2978	363	This work
[Ph ₂ PCS ₂]Tl(THF)Me ₂	2.17	168(1)	3.01	59.0	2347	350 ^a	^b
[Cy ₂ PCS ₂]TlMe ₂	—	—	—	—	2375	351	^b
[Pr ⁿ ₂ NCS ₂]TlMe ₂	2.18	153(1)	2.75	64.8	2941	—	^c
[Et ₂ PS ₂]TlMe ₂	2.13	169.7(6)	2.99	68.1	2313	351	^d
[Ph ₂ PS ₂]TlMe ₂	2.15	165.1	2.98	67.9	2268	350	^e
[MeOCS ₂]TlMe ₂	2.09	170.9	2.97	62.6	—	—	^f

^a The value listed in ref. 1 is 35 Hz, which is presumably a typographical error given the values for the other derivatives. ^b E. M. Vázquez-López, A. Sánchez, J. S. Casas, J. Sordo and E. E. Castellano, *J. Organomet. Chem.*, 1992, **438**, 29. ^c J. S. Casas, M. V. Castaño, C. Freire, A. Sánchez, J. Sordo, E. E. Castellano and J. Zukerman-Schpector, *Inorg. Chim. Acta*, 1994, **216**, 15. ^d R. Carballo, J. S. Casas, E. E. Castellano, A. Sánchez, J. Sordo, E. M. Vázquez-López and J. Zukerman-Schpector, *Polyhedron*, 1997, **16**, 3609. ^e J. S. Casas, A. Sánchez, J. Sordo, E. M. Vázquez-López, E. E. Castellano and J. Zukerman-Schpector, *Polyhedron*, 1992, **11**, 2889. ^f W. Schwarz, G. Mann and J. Weidlein, *J. Organomet. Chem.*, 1976, **122**, 303.

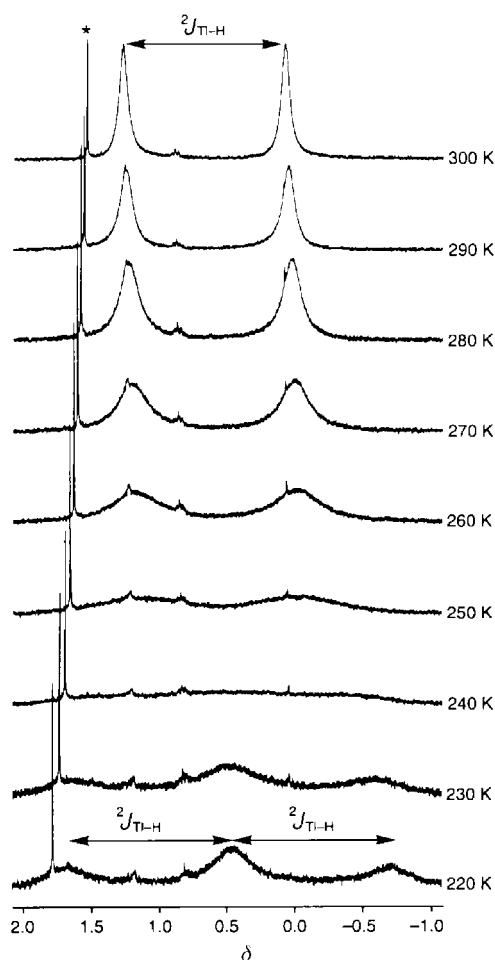
Table 2 Average E–C bond lengths and C–E–C bond angles for dimethyl derivatives of boron, aluminium, gallium, indium and thallium (taken from ref. 15)

E	<i>d</i> (E–Me)/Å	C–E–C°
B	1.62	112.3
Al	1.98	114.4
Ga	1.98	119.5
In	2.17	123.0
Tl	2.13	161.9

Furthermore, the S–Tl–S bond angle of 97.44(3)° for [pzBm^{Me}]TlMe₂ is substantially larger than has been observed for the other complexes listed in Table 1, which typically have S–Tl–S bond angles in the range 59–68°. Presumably these differences are a consequence of [pzBm^{Me}]TlMe₂ possessing an eight-membered chelate ring, whereas the other complexes listed in Table 1 possess four-membered chelate rings.

In accord with the solid state structure, the thallium-methyl groups are chemically inequivalent in the low temperature (220 K) ¹H NMR spectrum (Fig. 4); thus, two overlapping doublets are observed at δ –0.15 and 1.10 with ²*J*_{Tl–H} coupling constants of ca. 383 Hz.¹⁹ Upon warming, however, the two doublets coalesce, giving rise to a single doublet at δ 0.60 with a ²*J*_{Tl–H} coupling constant of ca. 363 Hz at 300 K.²⁰ Likewise the methyl groups are characterized by a doublet with a ¹*J*_{Tl–C} coupling constant of 2978 Hz in the room temperature ¹³C NMR spectrum. These values of ²*J*_{Tl–H} and ¹*J*_{Tl–C} compare favorably with those for the other thallium dimethyl complexes listed in Table 1.²¹

The fluxionality within [pzBm^{Me}]TlMe₂ involves exchange of the positions of the axial and equatorial thallium methyl ligands of the “chair-like” structure. However, such a process does not simply involve inversion of the “chair”, since that would also interchange the position of the pyrazolyl and hydrogen substituents on boron.²² Possible exchange mechanisms involve (i) dissociation of one of the sulfur donors followed by rotation of the TlMe₂ group about the remaining Tl–S bond, and (ii) coordination of the pyrazolyl group and Berry pseudorotation within the resulting five-coordinate intermediate. Analysis of the fluxional process, however, is complicated due to the fact that the NMR spectroscopic line widths are influenced by thallium nuclear relaxation *via* chemical shift anisotropy, which is strongly temperature dependent and increases markedly as the temperature is lowered.²³ Thus, the resonances attributable to the methyl groups are broad at low temperature, even in the absence of exchange. After compensation for line broadening due to thallium relaxation, an Eyring plot of the rate constant data over the temperature range 220 K–300 K (Table 3 and Fig. 5) gives rise to the activation parameters Δ*H*[‡] = 6.6(2) kcal mol^{–1} and Δ*S*[‡] = –17(1) e.u. for the fluxional process, although the mechanism of the fluxionality remains unknown.

**Fig. 4** Variable temperature ¹H NMR spectra of the thallium-methyl region of [pzBm^{Me}]TlMe₂ in CD₂Cl₂ (* = impurity).

(ii) Synthesis and structural characterization of {[Tm^{Ph}]Tl}₂ and {[Tm^{Ph}]Tl}[ClO₄]

The thallium(i) complex {[Tm^{Ph}]Tl}₂ is readily obtained by reaction of the lithium derivative [Tm^{Ph}]Li⁴ with Tl(O₂CMe), as illustrated in Scheme 2. {[Tm^{Ph}]Tl}₂ has been structurally characterized by X-ray diffraction (Fig. 6), thereby demonstrating that the complex exists with a dinuclear structure which resembles aspects of that for the bis(mercaptopomethylimidazoly)borate derivative, {[Bm^{Me}]Tl}₂.⁸ The dinuclear nature of {[Tm^{Ph}]Tl}₂ contrasts sharply with the structures of its [Tp^{RR}]-Tl counterparts, each of which exist as monomeric complexes with symmetrically coordinated tridentate tris(pyrazolyl)borate ligands.⁵

In addition to the thallium(i) complex, {[Tm^{Ph}]Tl}₂, the red-orange thallium(iii) species {[Tm^{Ph}]Tl₃}[ClO₄]₃ may be obtained by reaction of [Tm^{Ph}]Li with Tl(ClO₄)₃ (Scheme 2). The

molecular structure of $\{[\text{Tm}^{\text{Ph}}]_2\text{Ti}\}[\text{ClO}_4]$ has been determined by X-ray diffraction, as illustrated in Fig. 7, and the structure of the cation is similar to that in $\{[\text{Tm}^{\text{Me}}]_2\text{Ti}\}[\text{TiL}_4]$, which has been recently reported by Reglinski *et al.*^{24,25} For example, the average Ti–S bond lengths in $\{[\text{Tm}^{\text{Ph}}]_2\text{Ti}\}^+$ and $\{[\text{Tm}^{\text{Me}}]_2\text{Ti}\}^+$ are identical (2.69 Å). It is also noteworthy that the Ti–S bond lengths in these mercaptoimidazolylborate Ti^{III} complexes, namely $\{[\text{Tm}^{\text{Ph}}]_2\text{Ti}\}^+$, $\{[\text{Tm}^{\text{Me}}]_2\text{Ti}\}^+$ and $[\text{pzBm}^{\text{Me}}]\text{TiMe}_2$, are considerably shorter than the corresponding values for the other Ti^{III} complexes listed in Table 1.

Table 3 Rate constant data for $[\text{pzBm}^{\text{Me}}]\text{TiMe}_2$

T/K	k/s^{-1}
220	261
230	446
240	882
250	1540
260	2460
270	4140
280	6890
290	12800
300	19800

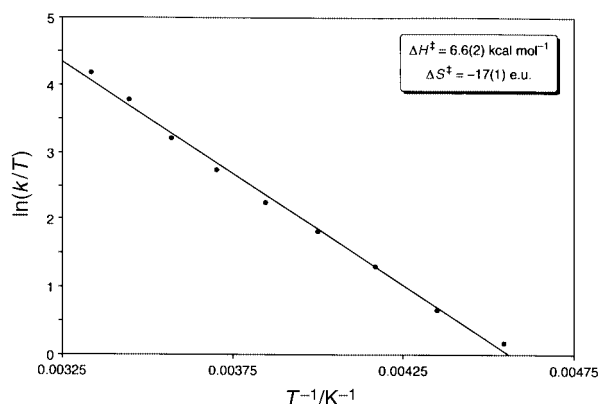


Fig. 5 Eyring plot for the fluxional process within $[\text{pzBm}^{\text{Me}}]\text{TiMe}_2$.

Interestingly, the ^1H NMR spectra of solutions of $\{[\text{Tm}^{\text{Ph}}]_2\text{Ti}\}[\text{ClO}_4]$ are *not* in accord with the solid state structure. Specifically, the ^1H NMR spectra of $\{[\text{Tm}^{\text{Ph}}]_2\text{Ti}\}[\text{ClO}_4]$ in $(\text{CD}_3)_2\text{CO}$, CDCl_3 , and $(\text{CD}_3)_2\text{SO}$ indicate the presence of two distinct types of $[\text{Tm}^{\text{Ph}}]$ ligands. For example, the two protons of the mercaptoimidazolyl nucleus are characterized by *four* sets of resonances in a 1:1:1:1 ratio at δ 7.26, 7.31, 7.34 and 7.44 ppm in DMSO (see Table 5). Furthermore, two resonances in the ratio 1:1 are observed at δ 2.58 and 2.94 ppm for the B–H moieties. The ^1H NMR spectra are also highly temperature dependent, as illustrated in Fig. 8 for a sample in $(\text{CD}_3)_2\text{CO}$. For example, at room temperature, the ^1H NMR spectrum exhibits in the range δ 7.2–7.4 ppm four sets of resonances, *i.e.* two sets of “AB” quartets, corresponding to the presence of two different $[\text{Tm}^{\text{Ph}}]$ fragments. The temperature dependence of the chemical shifts of one of these fragments is such that a “singlet” begins to emerge at 300 K. One plausible explanation

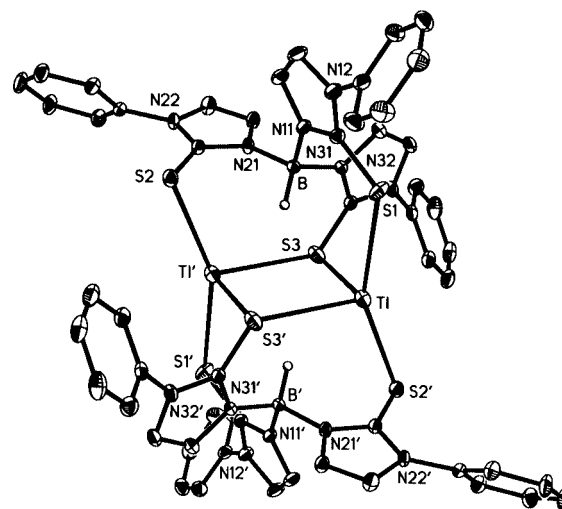
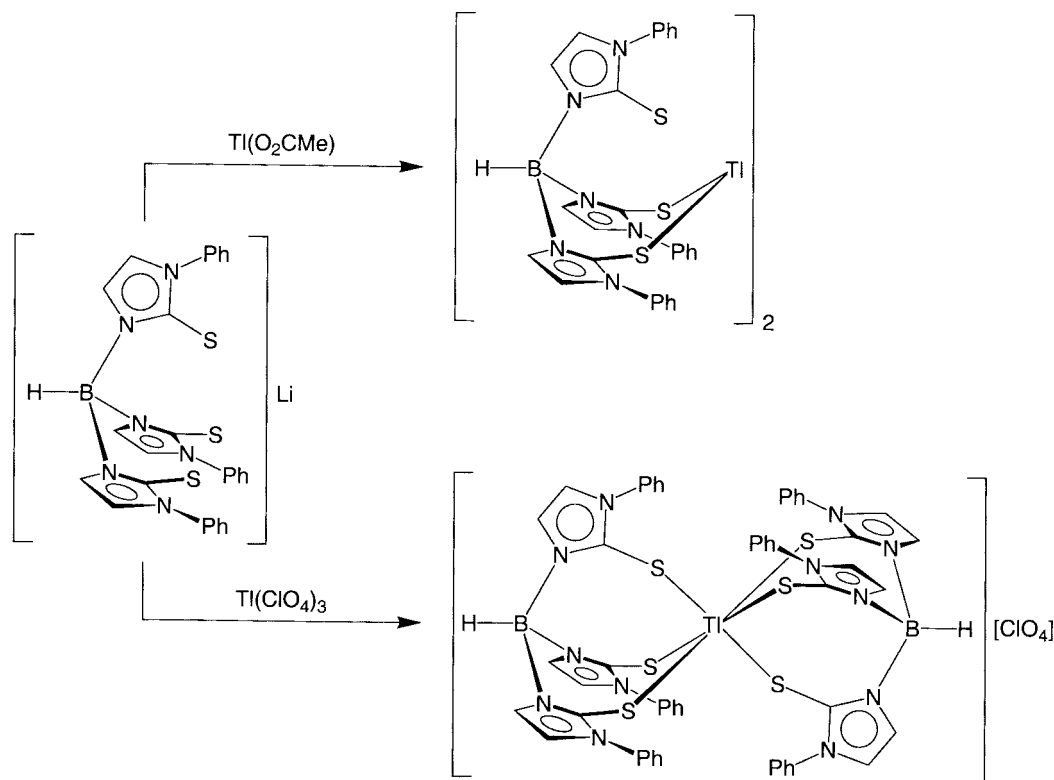


Fig. 6 Molecular structure of $\{[\text{Tm}^{\text{Ph}}]_2\text{Ti}\}_2$. Selected bond lengths (Å) and angles ($^\circ$): Ti–S(1) 3.396(1), Ti–S(2') 3.173(1), Ti–S(3) 3.049(1), Ti–S(3') 3.155(1), Ti \cdots H(1) 3.13(3); S(3)–Ti–S(3') 95.76(3), Ti–S(3)–Ti' 84.24(3).



Scheme 2

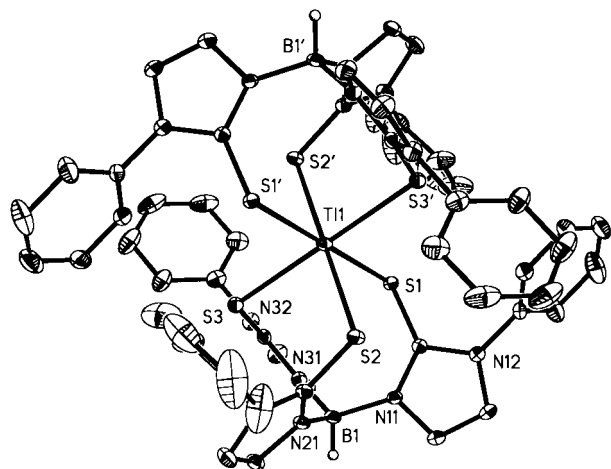


Fig. 7 Molecular structure of $\{[Tm^{Ph}]_2Ti\}[ClO_4]$ (only one of the independent molecules shown). Selected bond lengths (Å) and angles ($^\circ$): Ti(1)–S(1) 2.695(1), Ti(1)–S(2) 2.676(1), Ti(1)–S(3) 2.674(1), Ti(2)–S(4) 2.679(1), Ti(2)–S(5) 2.699(1), Ti(2)–S(6) 2.693(1); S(1)–Ti(1)–S(2) 90.61(4), S(1)–Ti(1)–S(2') 89.39(4), S(1)–Ti(1)–S(3) 92.05(3), S(1)–Ti(1)–S(3') 87.95(3), S(2)–Ti(1)–S(3) 89.55(4), S(2)–Ti(1)–S(3') 90.45(4), S(4)–Ti(2)–S(5) 92.09(4), S(4)–Ti(2)–S(5') 87.91(4), S(4)–Ti(2)–S(6) 91.15(4), S(4)–Ti(2)–S(6') 88.85(4), S(5)–Ti(2)–S(6) 92.12(4), S(5)–Ti(2)–S(6') 87.88(4).

for the NMR spectroscopic behavior is that dissociation of one of the $[Tm^{Ph}]$ ligands occurs in solution, generating a 1:1 mixture of $\{[Tm^{Ph}]Ti(solv.)\}^{2+}$ and $\{[Tm^{Ph}](solv.)\}^-$, which do not exchange rapidly on the NMR timescale.

Experimental

General considerations

All manipulations were performed using a combination of glovebox, high-vacuum or Schlenk techniques.²⁶ Solvents were purified and degassed by standard procedures. NMR spectra were recorded on Bruker Avance 300wb DRX, Bruker Avance 400 DRX, and Bruker Avance 500 DMX spectrometers. 1H and ^{13}C chemical shifts are reported in ppm relative to $SiMe_4$ ($\delta = 0$) and were referenced internally with respect to the protio solvent impurity or the ^{13}C resonances, respectively. All coupling constants are reported in Hz. IR spectra were recorded as KBr pellets on Perkin-Elmer 1430 or 1600 spectrophotometers and are reported in cm^{-1} . C, H, and N elemental analyses were measured using a Perkin-Elmer 2400 CHN Elemental Analyzer. FAB+ mass spectra were obtained using a 3-nitrobenzyl alcohol matrix and a JEOL HX 110HF mass spectrometer. $[pzBm^{Me}]Li^6$ and $[Tm^{Ph}]Li^4$ were prepared as previously reported.

Synthesis of $[pzBm^{Me}]Ti$

A solution of $Ti(O_2CMe)$ (3.5 g, 13.0 mmol) in MeOH (40 mL) was treated with $[pzBm^{Me}]Li$ (2.6 g, 10.6 mmol). The resulting suspension was stirred for 2.5 hours, after which the volatile components were removed *in vacuo*. The solid obtained was washed with H_2O (ca. 150 mL) and dried *in vacuo*, giving $[pzBm^{Me}]Ti$ as a white solid (3.5 g, 75%). IR data (KBr disk, cm^{-1}): 3418 (vw), 3129 (w), 3075 (w), 2938 (w), 2403 (w), 1558 (m), 1498 (m), 1453 (vs), 1405 (s), 1374 (vs), 1297 (vs), 1198 (vs), 1161 (m), 1114 (vs), 1096 (vs), 1075 (s), 1039 (s), 1002 (w), 960 (w), 918 (w), 878 (vw), 842 (vw), 762 (vs), 730 (vs), 703 (w), 690 (m), 679 (m), 622 (w), 610 (w), 518 (m), 468 (vw), 452 (w). NMR spectroscopic data are listed in Table 4.

Synthesis of $[pzBm^{Me}]ZnMe$

A suspension of $[pzBm^{Me}]Ti$ (3.0 g, 5.9 mmol) in benzene (100 mL) was treated with Me_2Zn (8.3 mL of a 2 M solution in

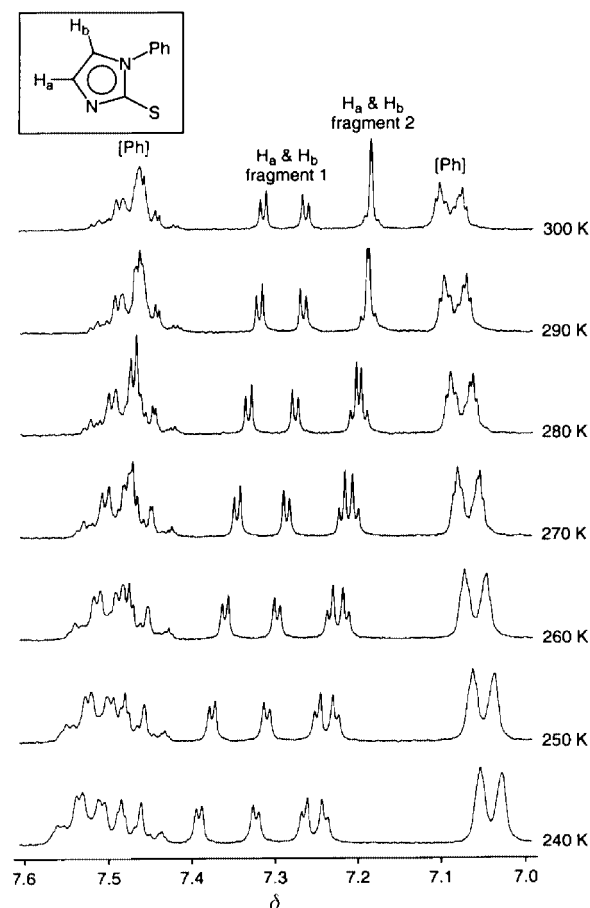


Fig. 8 Variable temperature 1H NMR spectra of $\{[Tm^{Ph}]_2Ti\}[ClO_4]$ in $(CD_3)_2CO$ (only the mercaptoimidazolyl residues are shown).

toluene, 16.6 mmol). The mixture was stirred for ten minutes at room temperature, resulting in the deposition of a black precipitate which was separated by filtration. The filtrate was concentrated and allowed to stand overnight, thereby depositing microcrystals. The supernatant was decanted and the residue washed with pentane (ca. 10 mL) and dried *in vacuo*, yielding $[pzBm^{Me}]ZnMe$ as a white powder (0.63 g, 28%). Analysis calculated for $[pzBm^{Me}]ZnMe$: C, 37.4%; H, 4.4%; N, 21.8%. Found: C, 37.4%; H, 3.9%; N, 21.8%. IR data (KBr disk, cm^{-1}): 3150 (m), 3123 (m), 3102 (m), 2941 (m), 2904 (m), 2830 (m), 2512 (w), 2474 (m), 2232 (w), 1570 (m), 1558 (m), 1509 (m), 1459 (s), 1418 (s), 1381 (s), 1304 (s), 1229 (s), 1201 (vs), 1149 (m), 1122 (m), 1086 (m), 1069 (s), 1037 (w), 1006 (w), 984 (w), 898 (vw), 864 (vw), 845 (vw), 780 (s), 762 (s), 739 (s), 699 (m), 687 (w), 671 (m), 647 (m), 524 (m), 470 (vw), 442 (w). NMR spectroscopic data are listed in Table 4.

Synthesis of $[pzBm^{Me}]TiMe_2$

A suspension of $[pzBm^{Me}]Ti$ (300 mg, 0.59 mmol) in acetone (15 mL) was treated with $TiMe_2Cl^{27}$ (175 mg, 0.65 mmol). The mixture was stirred for ca. 2 hours and filtered. The residue was extracted into chloroform and the mixture was filtered. The solvent was removed from the chloroform filtrate *in vacuo*, and the product was washed with pentane (ca. 10 mL) giving $[pzBm^{Me}]TiMe_2$ as a white solid (54 mg, 17%). Analysis calculated for $[pzBm^{Me}]TiMe_2$: C, 28.9%; H, 3.7%; N, 15.6%. Found: C, 29.0%; H, 3.5%; N, 15.8%. IR data (KBr disk, cm^{-1}): 3146 (w), 3138 (m), 3107 (w), 2999 (w), 2922 (m), 2531 (m), 2298 (w), 1562 (m), 1504 (w), 1455 (s), 1401 (m), 1374 (vs), 1319 (m), 1288 (s), 1189 (vs), 1158 (w), 1113 (s), 1089 (s), 1043 (m), 953 (w), 886 (m), 772 (m), 740 (s), 722 (s), 690 (w), 650 (vw), 624 (vw), 517 (vw), 464 (vw), 442 (vw). NMR spectroscopic data are listed in Table 4.

Table 4 NMR spectroscopic data for {pz[Bm^{Me}]M} derivatives (ppm, J/Hz)

	[pzBm ^{Me}]Tl ^a	[pzBm ^{Me}]ZnMe ^b	[pzBm ^{Me}]TlMe ₂ ^c
¹ H NMR			
HB{(C ₃ N ₂ H ₂ CH ₃ S) ₂ (C ₃ N ₂ H ₃)}	3.43, s [6H]	3.60, s	3.61, s
HB{(C ₃ N ₂ H ₂ CH ₃ S) ₂ (C ₃ N ₂ H ₃)}	6.33, d, ³ J _{H-H} = 2 [2H]	6.72, d, ³ J _{H-H} = 2 [2H]	6.70, d, ³ J _{H-H} = 2 [2H]
	6.93, d, ³ J _{H-H} = 2 [2H]	6.76, d, ³ J _{H-H} = 2 [2H]	7.41, d, ³ J _{H-H} = 2 [2H]
HB{(C ₃ N ₂ H ₂ CH ₃ S) ₂ (C ₃ N ₂ H ₃)}	6.10, t, ³ J _{H-H} = 2 [1H]	6.32, t, ³ J _{H-H} = 2 [1H]	6.19, t, ³ J _{H-H} = 2 [1H]
	7.44, d, ³ J _{H-H} = 2 [1H]	7.72, d, ³ J _{H-H} = 2 [1H]	7.66, d, ³ J _{H-H} = 2 [1H]
	7.54, d, ³ J _{H-H} = 2 [1H]	7.76, d, ³ J _{H-H} = 2 [1H]	7.78, d, ³ J _{H-H} = 2 [1H]
HB{(C ₃ N ₂ H ₂ CH ₃ S) ₂ (C ₃ N ₂ H ₃)}	5.32, broad	4.42, broad	Not observed
M-CH ₃		-0.63, s	0.80, d, ² J _{Tl-H} = 360
¹³ C NMR			
HB{(C ₃ N ₂ H ₂ CH ₃ S) ₂ (C ₃ N ₂ H ₃)}	33.9, q, ¹ J _{C-H} = 136	35.9, q, ¹ J _{C-H} = 141	34.1, q, ¹ J _{C-H} = 140
HB{(C ₃ N ₂ H ₂ CH ₃ S) ₂ (C ₃ N ₂ H ₃)}	118.1, d, ¹ J _{C-H} = 196 [2C]	119.4, d, ¹ J _{C-H} = 195 [2C]	118.6, d, ¹ J _{C-H} = 196 [2C]
	119.7, d, ¹ J _{C-H} = 196 [2C]	123.4, d, ¹ J _{C-H} = 195 [2C]	120.5, d, ¹ J _{C-H} = 194 [2C]
	161.3, s [2C]	157.4, s [2C]	159.0, s [2C]
HB{(C ₃ N ₂ H ₂ CH ₃ S) ₂ (C ₃ N ₂ H ₃)}	103.3, d, ¹ J _{C-H} = 174 [1C]	105.4, d, ¹ J _{C-H} = 178 [1C]	103.4, d, ¹ J _{C-H} = 173 [1C]
	134.6, d, ¹ J _{C-H} = 196 [1C]	140.4, d, ¹ J _{C-H} = 188 [1C]	134.9, d, ¹ J _{C-H} = 182 [1C]
	139.5, d, ¹ J _{C-H} = 196 [1C]	142.5, d, ¹ J _{C-H} = 186 [1C]	139.6, d, ¹ J _{C-H} = 180 [1C]
M-CH ₃		-13.8, q, ¹ J _{C-H} = 119	19.5, dq, ² J _{Tl-C} = 2978 [2C]

^a In DMSO. ^b In CDCl₃. ^c ¹H NMR in CDCl₃ at 300 K; ¹³C NMR in DMSO.**Table 5** NMR spectroscopic data for {[Tm^{Pb}]M} derivatives (ppm, J/Hz)

	{[Tm ^{Pb}]Tl} ₂ ^a	{[Tm ^{Pb}] ₂ Tl}[ClO ₄] ^{a,b}
¹ H NMR		
HB{(C ₃ N ₂ H ₂ (C ₆ H ₅)S) ₃ }	7.37, t, ³ J _{H-H} = 8 (<i>para</i>) [3H] 7.48, t, ³ J _{H-H} = 8 (<i>meta</i>) [6H] 7.64, d, ³ J _{H-H} = 8 (<i>ortho</i>) [6H]	6.44, m [18H] 7.00, m [12H]
HB{(C ₃ N ₂ H ₂ (C ₆ H ₅)S) ₃ }	6.75, d, ³ J _{H-H} = 2 [3H] 7.26, d, ³ J _{H-H} = 2 [3H]	7.26, d (part. res.), [3H] 7.31, d (part. res.), [3H] 7.34, d (part. res.), [3H] 7.44, d (part. res.), [3H]
HB{(C ₃ N ₂ H ₂ (C ₆ H ₅)S) ₃ }	5.52, broad	2.58, broad [1H] 2.94, broad [1H]
¹³ C NMR		
HB{(C ₃ N ₂ H ₂ (C ₆ H ₅)S) ₃ }	126.2, d, ¹ J _{C-H} = 181 [6C] 127.3, d, ¹ J _{C-H} = 158 [3C] 128.5, d, ¹ J _{C-H} = 158 [6C] 138.6, s [3C]	127.5 [3C] 127.6 [3C] 128.5 [9C] 128.6 [3C] 136.6 [3C] 136.7 [3C] 153.5 [3C] 155.3 [3C]
HB{(C ₃ N ₂ H ₂ (C ₆ H ₅)S) ₃ }	118.5, d, ¹ J _{C-H} = 196 [3C] 121.5, d, ¹ J _{C-H} = 196 [3C] 162.9, s [3C]	122.1 [3C] 122.4 [3C] 125.3 [6C]

^a In DMSO. ^b The data listed are not intended to indicate to which of the two [Tm^{Pb}] fragments the resonances correspond.

Synthesis of {[Tm^{Pb}]Tl}₂

To a solution of Tl(O₂CMe) (3.55 g, 13.47 mmol) in MeOH (150 mL) was added [Tm^{Pb}]Li (3.66 g, 6.73 mmol). The mixture was stirred for 1 hour at room temperature, after which the methanol was removed *in vacuo*. The residue obtained was washed with water (*ca.* 500 mL) and dried *in vacuo*, giving [Tm^{Pb}]Tl as a white powder (4.56 g, 91%). Analysis calculated for Tl[Tm^{Pb}]: C, 43.7%; H, 3.0%; N, 11.3%. Found: C, 43.9%; H, 2.4%; N, 11.0%. IR data (KBr pellet, cm⁻¹): 3442 (w), 3109 (m), 3071 (m), 2957 (w), 2606 (w), 2444 (w), 1596 (m), 1557 (w), 1498 (vs), 1456 (w), 1415 (vs), 1352 (vs), 1309 (s), 1255 (s), 1188 (s), 1157 (s), 1093 (s), 1027 (m), 1002 (w), 956 (w), 910 (w), 834 (vw), 764 (s), 735 (s), 690 (vs), 632 (w), 608 (w), 582 (m), 569 (m), 528 (w), 508 (w). NMR spectroscopic data are listed in Table 5.

Synthesis of {[Tm^{Pb}]₂Tl}[ClO₄]

A suspension of [Tm^{Pb}]Li (0.50 g, 0.92 mmol) in methanol

(5 mL) was quickly treated with Tl(ClO₄)₃·xH₂O (0.22 g, 0.45 mmol for *x* = 0), resulting in the immediate formation of a red-orange precipitate. The mixture was allowed to stand at room temperature overnight and filtered. The precipitate was washed with methanol (10 mL), and extracted into CHCl₃ (3 × 5 mL). The volatile components were removed from the combined extracts giving {[Tm^{Pb}]₂Tl}[ClO₄] as a red-orange powder (0.18 g, *ca.* 30% based on [Tm^{Pb}]Li). FAB+ *m/z* = 1278 (*M*⁺ - H). IR data (KBr pellet, cm⁻¹): 3427 (w), 3137 (w), 2959 (w), 2420 (w), 2290 (vw), 2212 (vw), 1596 (s), 1554 (s), 1498 (vs), 1456 (m), 1427 (s), 1353 (vs), 1261 (s), 1189 (vs), 1147 (s), 1091 (vs), 1024 (s), 955 (m), 909 (w), 866 (vw), 801 (m), 758 (s), 732 (s). NMR spectroscopic data are listed in Table 5.

X-Ray structure determinations

Crystal data, data collection and refinement parameters are summarized in Table 6. X-Ray diffraction data for [pzBm^{Me}]-ZnMe were collected on a Siemens P4 diffractometer, while

Table 6 Crystal, intensity collection and refinement data

	[pzBm ^{Me}]ZnMe	[pzBm ^{Me}]TlMe ₂	{[Tm ^{Ph}]Tl} ₂ ·CHCl ₃	{[Tm ^{Ph}]Tl}[ClO ₄]
Lattice	Orthorhombic	Monoclinic	Triclinic	Triclinic
Formula	C ₁₂ H ₁₇ BN ₆ S ₂ Zn	C ₁₃ H ₂₀ BN ₆ S ₂ Tl	C ₃₅ H ₄₅ B ₂ Cl ₃ N ₁₂ S ₆ Tl ₂	C ₅₄ H ₄₄ B ₂ ClN ₁₂ O ₄ S ₆ Tl
Formula weight	385.62	539.65	1603.10	1378.81
Space group	<i>Pbca</i> (no. 61)	<i>P2₁/n</i> (no. 14)	<i>P</i> $\bar{1}$ (no. 2)	<i>P</i> $\bar{1}$ (no. 2)
<i>a</i> /Å	14.683(1)	7.6486(4)	10.334(1)	11.848(1)
<i>b</i> /Å	12.170(1)	14.5166(7)	10.639(1)	12.074(1)
<i>c</i> /Å	18.895(3)	16.9156(8)	14.801(1)	22.124(1)
<i>a</i> ^o			103.389(2)	90.296(1)
<i>β</i> ^o		101.822(1)	95.630(2)	97.423(1)
<i>γ</i> ^o			100.605(2)	109.724(1)
<i>V</i> /Å ³	3376.2(7)	1838.3(2)	1539.2(2)	2950.1(3)
<i>Z</i>	8	4	1	2
Temperature/K	298	203	243	228
<i>μ</i> (Mo-Kα)/mm ^{−1}	1.705	9.019	5.609	3.050
No. of data	2942	4224	6814	12786
No. of parameters	206	217	384	725
<i>R</i> ₁	0.0449	0.0228	0.0384	0.0354
<i>wR</i> ₂	0.0966	0.0557	0.0559	0.1080

data for [pzBm^{Me}]TlMe₂, {[Tm^{Ph}]Tl}₂ and {[Tm^{Ph}]Tl}[ClO₄] were collected on a Bruker P4 diffractometer equipped with a SMART CCD detector. The structures were solved using direct methods and standard difference map techniques, and were refined by full-matrix least-squares procedures using SHELXTL.²⁸

CCDC reference number 186/1878.

See <http://www.rsc.org/suppdata/dt/a9/a909542j/> for crystallographic files in .cif format.

Dynamic NMR experiments

The fluxional process within [pzBm^{Me}]TlMe₂ was analyzed by using gNMR.²⁹ However, such an analysis requires knowledge of the natural NMR spectroscopic line width in the absence of exchange, which itself is temperature dependent due to the effect of thallium relaxation (*vide supra*). In order to account for the temperature dependence of the line width due to thallium relaxation, the Tl relaxation times (*T*_{1(Tl)}) were estimated at each temperature by consideration of the thallium relaxation data for the related tris(pyrazolyl)hydroborato complex, [Tp^{Bu}]Tl.²³ From these data, estimates for the contribution to natural line width (*ca.* 10 Hz) in the ¹H NMR spectrum due to thallium relaxation, *i.e.* 1/{2π*T*_{1(Tl)}},³⁰ at each temperature are: 220 K (25 Hz), 230 K (18 Hz), 240 K (15 Hz), 250 K (12 Hz), 260 K (10 Hz), 270 K (9 Hz), 280 K (7 Hz), 290 K (6 Hz), 300 K (5 Hz). The rate constant data is presented in Table 3, with an Eyring plot in Fig. 5 (Δ*H*[‡] = 6.6(2) kcal mol^{−1} and Δ*S*[‡] = −17(1) e.u.).

Conclusion

In summary, mercaptoimidazolylborate ligands have been used to prepare complexes of both Tl^I and Tl^{III}. The thallium(III) complexes, [pzBm^{Me}]TlMe₂ and {[Tm^{Ph}]Tl}[ClO₄], are particularly interesting since poly(pyrazolyl)borate counterparts have not been isolated and structurally characterized. The structure of [pzBm^{Me}]TlMe₂ is also noteworthy since the pyrazolyl group of the [S₂N] hybrid ligand does not interact with the thallium center, which is therefore four-coordinate rather than five-coordinate. In contrast, all the mercaptoimidazolyl groups interact with the six-coordinate thallium center of {[Tm^{Ph}]Tl}₂⁺. These observations suggest that Tl^{III} has a greater tendency to bind sulfur donors over nitrogen donors.

Acknowledgements

We thank the National Science Foundation (CHE 96-10497) for support of this research. The referees are thanked for helpful comments.

References

- 1 Bis- and tris-(pyrazolyl)hydroborato ligands are represented by the abbreviations [Bp^{RR'}] and [Tp^{RR'}], with the 3- and 5-alkyl substituents listed respectively as superscripts. A substituent (X) on boron other than hydrogen is listed as a prefix, *i.e.* [XBp^{RR'}] and [XTp^{RR'}]. By analogy, we use the abbreviations [Bm^R] and [Tm^R] to represent the bis(2-mercapto-1-alkylimidazolyl)borate and tris(2-mercapto-1-alkylimidazolyl)borate ligands, respectively.
- 2 M. Garner, J. Reglinski, I. Cassidy, M. D. Spicer and A. R. Kennedy, *Chem. Commun.*, 1996, 1975.
- 3 For other studies using the [Tm^{Me}] ligand, see: (a) C. Santini, C. Pettinari, G. G. Lobbia, R. Spagna, M. Pellei and F. Vallorani, *Inorg. Chim. Acta*, 1999, **285**, 81; (b) C. Santini, G. G. Lobbia, C. Pettinari, M. Pellei, G. Valle and S. Calogero, *Inorg. Chem.*, 1998, **37**, 890; (c) J. Reglinski, M. D. Spicer, M. Garner and A. R. Kennedy, *J. Am. Chem. Soc.*, 1999, **121**, 2317; (d) A. F. Hill, G. R. Owen, A. J. P. White and D. J. Williams, *Angew. Chem., Int. Ed.*, 1999, **38**, 2759.
- 4 C. Kimblin, B. M. Bridgewater, D. G. Churchill and G. Parkin, *Chem. Commun.*, 1999, 2301.
- 5 For recent reviews, see: (a) S. Trofimenko, *Scorpionates—The Coordination Chemistry of Polypyrazolylborate Ligands*, Imperial College Press, London, 1999; (b) C. Janiak, *Main Group Met. Chem.*, 1998, **21**, 33; (c) D. L. Reger, *Coord. Chem. Rev.*, 1996, **147**, 571; (d) G. Parkin, *Adv. Inorg. Chem.*, 1995, **42**, 291; (e) S. Trofimenko, *Chem. Rev.*, 1993, **93**, 943; (f) N. Kitajima and W. B. Tolman, *Prog. Inorg. Chem.*, 1995, **43**, 419; (g) I. Santos and N. Marques, *New J. Chem.*, 1995, **19**, 551; (h) M. Etienne, *Coord. Chem. Rev.*, 1997, **156**, 201; (i) P. K. Byers, A. J. Canty and R. T. Honeyman, *Adv. Organomet. Chem.*, 1992, **34**, 1.
- 6 C. Kimblin, T. Hascall and G. Parkin, *Inorg. Chem.*, 1997, **36**, 5680.
- 7 See, for example, ref. 6 and references therein.
- 8 C. Kimblin, B. M. Bridgewater, T. Hascall and G. Parkin, *J. Chem. Soc., Dalton Trans.*, 2000, 891.
- 9 A. Looney, R. Han, I. B. Gorrell, M. Cornebise, K. Yoon, G. Parkin and A. L. Rheingold, *Organometallics*, 1995, **14**, 274.
- 10 R. Alsasser, A. K. Powell, S. Trofimenko and H. Vahrenkamp, *Chem. Ber.*, 1993, **126**, 685.
- 11 J. L. Kisko, T. Fillebeen, T. Hascall and G. Parkin, *J. Organomet. Chem.*, 2000, **596**, 22.
- 12 For theoretical studies of the disproportionation reactions of Tl^I complexes, see: (a) P. Schwerdtfeger, G. A. Heath, M. Dolg and M. A. Bennett, *J. Am. Chem. Soc.*, 1992, **114**, 7518; (b) P. Schwerdtfeger, P. D. W. Boyd, G. A. Bowmaker, H. G. Mack and H. Oberhammer, *J. Am. Chem. Soc.*, 1989, **111**, 15.
- 13 H. Gilman and R. G. Jones, *J. Am. Chem. Soc.*, 1946, **68**, 517.
- 14 Cambridge Structural Database (Version 5.17), *3D Search and Research Using the Cambridge Structural Database*, F. H. Allen and O. Kennard, *Chemical Des. Automat. News*, 1993, **8**, 1 & 31–37.
- 15 See, for example: C. Dowlin and G. Parkin, *Polyhedron*, 1999, **18**, 3567 and references therein.
- 16 D. L. Reger, S. J. Knox, A. L. Rheingold and B. S. Haggerty, *Organometallics*, 1990, **9**, 2581.
- 17 [pzBp]TlR₂ (R = Et, Buⁿ) complexes have been prepared by reaction of Na[Bpz₄] with R₂TlBr, but have not been structurally

- characterized. See: M. Onishi, K. Hiraki and S. Nakagawa, *Bull. Chem. Soc. Jpn.*, 1980, **53**, 1459.
- 18 For further comparison, the mean Tl–S bond length for complexes listed in the Cambridge Structural Database (Version 5.17) is 2.92 Å, with a range of 2.47–3.48 Å.
 - 19 Thallium exists as two naturally occurring spin 1/2 isotopes: ^{203}Tl (29.5%, $\gamma = 1.554 \times 10^8 \text{ rad T}^{-1} \text{ s}^{-1}$) and ^{205}Tl (70.5%, $\gamma = 1.569 \times 10^8 \text{ rad T}^{-1} \text{ s}^{-1}$). Due to the similarity of their gyromagnetic ratios, the difference in ^{203}Tl and ^{205}Tl coupling constants is generally not discernible [$J(^{205}\text{Tl}-\text{X}) = 1.0097(J^{203}\text{Tl}-\text{X})$]. See, for example: M. S. Garcia-Tasende, M. I. Suárez, A. Sánchez, J. S. Casas, J. Sordo, E. E. Castellano and Y. P. Mascarenhas, *Inorg. Chem.*, 1987, **26**, 3818.
 - 20 For comparison, the $^2J_{\text{Tl-H}}$ coupling constants for $[\text{pz}_2\text{Bp}]\text{TlEt}_2$ and $[\text{pz}_2\text{Bp}]\text{TlBu}^n$ are 306 Hz and 338 Hz, respectively. See ref. 17.
 - 21 For further comparison, $^1J_{\text{Tl-C}}$ and $^2J_{\text{Tl-H}}$ coupling constants for other Me_2TlX derivatives (e.g. $\text{X} = \text{Cl}, \text{I}, \text{NO}_3, \text{OPh}, \text{ClO}_4, \text{acac}$) are in the range 2475–2971 Hz and 336–471 Hz, respectively, in a variety of solvents. See: (a) P. J. Burke, R. W. Matthews and D. G. Gillies, *J. Organomet. Chem.*, 1976, **118**, 129; (b) Y. Kawasaki and M. Aritomi, *J. Organomet. Chem.*, 1976, **104**, 39.
 - 22 Alternatively, the NMR spectroscopic exchange data is in accord with a simple inversion process if the chemical shift of the thallium methyl protons depend only on whether the methyl group is located axially or equatorially and is independent of whether the boron pyrazolyl group occupies an axial or equatorial position.
 - 23 P. Ghosh, P. J. Desrosiers and G. Parkin, *J. Am. Chem. Soc.*, 1998, **120**, 10416.
 - 24 P. A. Slavin, J. Reglinski, M. D. Spicer and A. R. Kennedy, *J. Chem. Soc., Dalton Trans.*, 2000, 239.
 - 25 Reglinski has also reported a six-coordinate bismuth(III) sandwich species as a component of the novel salt $\{[\text{Tm}^{\text{Me}}]_2\text{Bi}\}\{[\text{Tp}]_2\text{Na}\}$. See ref. 3(c).
 - 26 (a) J. P. McNally, V. S. Leong and N. J. Cooper, in *Experimental Organometallic Chemistry*, eds. A. L. Wayda and M. Y. Darensbourg, American Chemical Society, Washington, DC, 1987, ch. 2, pp. 6–23; (b) B. J. Burger and J. E. Bercaw, in *Experimental Organometallic Chemistry*, eds. A. L. Wayda and M. Y. Darensbourg, American Chemical Society, Washington, DC, 1987, ch. 4, pp. 79–98; (c) D. F. Shriver and M. A. Drezdson, *The Manipulation of Air-Sensitive Compounds*, 2nd edn., Wiley-Interscience, New York, 1986.
 - 27 I. E. Markó and J. M. Southern, *J. Org. Chem.*, 1990, **55**, 3368.
 - 28 G. M. Sheldrick, SHELXTL, An integrated system for solving, refining and displaying crystal structures from diffraction data, University of Göttingen, Göttingen, Federal Republic of Germany, 1981.
 - 29 gNMR (Version 4.1), Cherwell Scientific Ltd., Oxford, 1995.
 - 30 F. Brady, R. W. Matthews, M. J. Forster and D. G. Gillies, *J. Chem. Soc., Chem. Commun.*, 1981, 911.